Chapter 3

Simulation of Pulsar population

3.1 Introduction

One of the important conclusions we arrived at in the previous chapter is that a fraction of solitary pulsars may, in fact, be recycled pulsars from binary systems which disrupted during the second explosion. Our estimate suggested that this fraction could be as large as $10 - 15\%$. In this Chapter we undertake an independent study to check and constrain these conclusions. The approach we adopt is the one of Monte Carlo simulation.

In this simulation a large number of binary systems and single stars are generated, and with some simplified assumptions on the evolution of stars in binary systems, their final products are determined. This helps one to determine the relative importance of pulsars coming from various kinds of progenitors. In addition to the aim of finding the fraction of recycled pulsars, this simulation has helped to estimate the formation rate of double neutron star binaries and their merger rate (due to the emission of gravitational radiation) in the Galaxy, and the number of ***active*** (where at least one neutron star is functioning as pulsar) double neutron star binaries in the Galaxy. By assuming a spatial density of galaxies, the count rate of mergers upto a distance of $\sim 200\text{Mpc}$ has been calculated. This turns out to be about a few events per year. This number is quite important for sensitive gravitational wave detectors like LIGO.

The plan of this chapter is as follows. Section **3.2** gives the details of the assumptions made in simulating the neutron star population. The procedure which was followed in doing the simulation is described in section **3.3.** The results are summarised in section **3.4,** and the implications of these results are discussed in section 3.5.

3.2 Assumptions

3.2.1 Assumptions about the binary parameters

The *Initial Mass Function* for stars whose masses are greater than about $1M_{\odot}$ is assumed to be $\psi(M) = C_1 M^{-2.7}$, where C_1 is the normalisation constant (Scalo *1986).*

The *Initial Mass-Ratio Function* is assumed to be (Hogeveen 1990,1991),

$$\begin{aligned} \psi(q) &= K_1 && \text{when } 0.1 \leq q < 0.25 \\ \psi(q) &= K_2\, q^{-1.5} && \text{when } 0.25 \leq q \leq 1 \end{aligned} \tag{3.1}$$

here, $q = M_2/M_1$ where M_1 and M_2 are the primary and the secondary masses of the binary system, and K_1 and K_2 are the normalisation constants.

The *Initial semimajor axis* distribution is assumed to be uniform in a logarithmic scale. The semimajor axes are selected in such a way that the primary star overflows the Roche lobe after the ignition of Helium, but before the ignition of Carbon (it is essentially a modified method of Dewey & Cordes 1987). A fit was produced for this purpose, with the Stellar evolution model by Schaller et *al.* (1992). This fit gives the lower and upper limits of the Roche lobe radius of the primary star, as a function of its mass.

$$\log R_L = \kappa_1 + \kappa_2 \log M_1 \tag{3.2}$$

For the lower limit, $\kappa_1 = 0.29 \pm 0.02$ and $\kappa_2 = 0.68 \pm 0.02$, and for the upper limit, $\kappa_1 = 0.79 \pm 0.12$ and $\kappa_2 = 1.77 \pm 0.12$.

It is assumed that during the Roche lobe overflow, the primary star loses the whole of its envelope. A fraction of this mass is accreted onto the secondary star. and the rest is lost from the system. The fraction of mass that is lost from the system is modelled as a function of the mass-ratio (Pols et al. 1992). If q > 0.6 it is assumed that the whole of the mass that is lost by the primary is accreted onto the secondary, and if q < 0.2 it is assumed that no mass is accreted onto the secondary. For values of q in the range of 0.2 – 0.6, the fraction of mass lost from the system is calculated by a linear interpolation. The evolution of semimajor axis in this phase is computed according to the formula given by Bhattacharya & van den Heuvel (1991).

During the supernova explosion, whether or not the binary survives depends on the amount of mass lost from the system, and the magnitude and the direction of the asymmetric kick velocity. The binary disrupts if the following condition is satisfied (Flannery & van den Heuvel 1975; Hills 1983).

$$\Delta M \geq \frac{M_\circ}{2}\left[1 - \left(\frac{v_k}{v_c}\right)^2 - 2\left(\frac{v_\circ}{v_c}\right)\left(\frac{v_k}{v_c}\right)\cos\theta\right] \tag{3.3}$$

where v_k and θ are the magnitude of the kick velocity and the angle it makes with the pre-explosion reduced orbital velocity v,. $M_\circ$ is the total mass of the system and $v_c = \sqrt{GM_\circ/a_\circ}$. This reduces to the simple Newtonian result if $v_k = 0$. namely the binary disrupts if more than half the total mass is lost.

If the binary survives after the supernova explosion, the change in the semimajor axis is given by (Hills 1983),

$$\begin{aligned} \frac{a}{a_\circ} &= \left[\frac{1-(\Delta M/M_\circ)}{1-(2\Delta M/M_\circ)-Y^2}\right] \qquad (3.4) \\ \text{Where,} \quad Y^2 &= \left(\frac{v_k}{v_c}\right)^2 + 2\left(\frac{v_\circ}{v_c}\right)\left(\frac{v_k}{v_c}\right)\cos\theta \end{aligned}$$

During the Roche lobe overflow of the primary star the mass of the secondary star gets modified. Because of this, the evolutionary timescales of the secondary gets altered. The **left-over** mainsequence timescale of the secondary is calculated by (van den Heuvel 1969),

$$T'_H = T_H(M_2)\left[1 - \frac{T_H(M_1^\circ)\; M_c(q_\circ M_1^\circ)}{T_H(q_\circ M_1^\circ)\; M_c(M_2)}\right] \qquad (3.5)$$

The threshold mass for the neutron star formation for solitary progenitors is assumed to be $8M_\odot$ (Hillebrandt 1987). In the case of helium stars, the minimum mass for neutron star formation is assumed to be $2.2M_\odot$ (Habets 1985,1986). For stars in binary systems, since they undergo extensive mass loss during their evolution the threshold mass gets pushed up. The threshold mass of these stars is assumed to be the main sequence mass corresponding to the helium star threshold mass (*i.e.,* $2.2M_\odot$) – $10M_\odot$.

The change in the semimajor axis during the common envelope phase during the Roche lobe overflow of the secondary star was computed with respect to the model suggested by Webbink(1984), and Bhattacharya and van den Heuvel(1991),

$$\frac{a}{a_\circ} = \left(\frac{M_1 M_{2c}}{M_{2c}+M_{2e}}\right)\left(\frac{1}{M_1 + 2M_{2e}/\lambda r_L}\right) \qquad (3.6)$$

where M_1 is the mass of the compact star (in our case, neutron star). M_{2c} and M_{2e} are the masses of the core and the envelope of the secondary star respectively.

$(a_\circ r_L)$ is the Roche lobe radius of the secondary star and λ is the weighting factor (< 1) for the gravitational binding energy of the core arid the envelope of the secondary star. For this exercise the value of λ was assumed to be 0.6. It is assumed that all binaries (irrespective of the mass-ratio and semimajor axis) go through this spiral-in phase, described by the above given equation.

A fit was produced to calculate the radius of stars in the main sequence on the basis of the stellar evolution model by Schaller et al. *(1992)*. If mass M and radius R are substituted in solar units, this fit is given by,

$$\log R = \alpha + \beta \log M \tag{3.7}$$

Mass range	α	β
$M \leq 1.5M$	$(7.741 \pm 3.602) \times 10^{-3}$	1.291 ± 0.035
$M > 1.5M$	0.140 ± 0.009	0.582 ± 0.007

Similarly, to calculate the radius R_c of the helium core of the stars as a function of the core mass M_c, a fit was produced on the basis of the Helium star evolution model by Habets *(1985)*. This fit is given by,

$$\log R_c = \zeta + \eta M_c \tag{3.8}$$

where $\zeta = -0.596$ and $\eta = 8.996 \times 10^{-2}$. After the primary overflow, if the semimajor axis is less than the sum of the main sequence radius of the modified secondary and the core radius of the primary, then the binary is assumed to give rise to one solitary neutron star. Similarly, after the spiral-in phase during the secondary star overflow (see equation *3.6)* if the semimajor axis is less than the radius of the core of the secondary, it is assumed that the system gives rise to only one neutron star, which will be a recycled one.

If the mass of the helium stars is relatively low, the outer helium shell expands to large radii during the late stages of evolution of a helium stars (Habets 1985).

This raises the possibility of these low mass helium stars going through a second stage of mass transfer (Case BB, or CB). This possibility is completely neglected in this exercise. The possible effect of this assumption is discussed in section 3.4.2.

3.2.2 Kick velocity distribution

It is suspected now a days that the supernova explosion may not be spherically symmetric. Because of this, the neutron star gets a kick in the opposite direction to the asymmetry, during its formation. At present there is no clear idea on what causes the asymmetry, and what is the distribution of the asymmetric kick velocities. For this work, two asymmetric kick velocity distributions were assumed. The first is by Hansen & Phinney (1996) (with the original functional form of Paczynski 1990), and the second, by Lyne & Lorimer (1993). The Hansen-Paczynski-Phinney (hereafter **HPP)** distribution is given by,

$$\psi(x)\,\mathrm{d}x \;=\; \frac{\mathrm{d}x}{(1+x^2)^2} \tag{3.9}$$

where x $= (v/v_\star)$ with $v_\star = 600$ km/sec. The Lyne & Lorimer distribution of velocities in two dimensions is given by,

$$\psi(x)\,\mathrm{d}x \;=\; \frac{x^{0.3}}{1+x^{3.3}}\,\mathrm{d}x \tag{3.10}$$

with v, $= 330$ km/sec. The results were checked for both the velocity distributions.

3.2.3 Beaming factor

As explained in Chapter 2, beaming factor is the fractional solid angle of the sky covered by the pulsar emission beam. In Chapter 2 it was assumed to be a constant of value 0.2. However, there are some models which suggest that the beaming factor could be period dependent (Narayan & Vivekanand 1983; Rankin 1990; Lyne, hlanchester & Taylor 1983). For this exercise the beaming factor is assumed to be the one given by Lyne & Manchester (1988),

$$f_b \propto P^{-1/3} \tag{3.11}$$

3.2.4 Field Decay Model

The magnetic fields of pulsars are assumed to decay according to the model given by Srinivasan et al. (1990). In this model the field decay is due to the expulsion of magnetic flux from the interior when the neutron star spins down during the course of evolution. The spin-down could be due to the dipole radiation, or due to the main sequence stellar wind from the companion in binary systems. If one assumes that the field resides in the core when the pulsar is born, according to this model the field evolution is governed by the following set of coupled differential equations.

$$\begin{aligned}
\frac{\dot{B}_{co}}{B_{co}} &= -\frac{\dot{P}}{P} \\
\dot{B}_{cr} &= -\left(\dot{B}_{co} + \frac{B_{cr}}{\tau_d}\right) \\
\dot{P} &= \frac{(B_{co} + B_{cr})^2}{K\,P} \\
\text{where K} &= \left(\frac{3Ic^3}{8\pi^2 R_n^6}\right)
\end{aligned} \tag{3.12}$$

Here, B_{co} and B_{cr} are the core and the crustal fields, **P** is the rotation period of the pulsar, and τ_d is the field decay time scale in the crust. **I** and R_n are the moment of inertia and the radius of the neutron star, and c is the velocity of light.

The decay time scale in the core is assumed to be infinity, since the matter in the interior is believed to be super conducting. However, the decay time scale in the crust is assumed to be 100 Myr (Bhattacharya et al. 1992). The first equation in the above set of equations comes from the work of Srinivasan et al. (1990), that the amount of core field deposited at the crust is directly proportional to the extent to which pulsar's rotation has been slowed down. The second equation gives the change in the crust field. The first term gives the contribution from the core field, and the second term accounts for the decay of the crustal field due to ohmic dissipation. The third equation is the familier dipole formula, where the field strength is related to the rotation period and its time derivative. To account for the field decay by the dipole spin-down, the above given equations were numerically solved by Runge-Kutta method (Press et al. 1994).

However, when a neutron star is born in a binary system, it is believed that the mild wind from the main sequence companion can slow down the neutron star. Therefore, to account for the field decay when the neutron star is in a binary system, the equation for **P** in equation **3.12** must be replaced by (Illarianov & Sunyaev 1975),

$$\dot{P} = \frac{P^2 \dot{m} R_A}{2\pi I}\left[\frac{2\pi R_A}{P} - \sqrt{\frac{G\,M_n}{R_A}}\right] \tag{3.13}$$

here, R_A is the Alfvén radius', and m is the mass intercepted by the accretion radius of the neutron star from the main sequence companion. The main sequence stellar wind rate M_s was calculated by using a fit by De Jagar, Nieuwenhuijzen

'Alfven radius is defined as the radius at which the energy density of the magnetic field equals the kinetic energy density of the infalling plasma (stellar wind from the companion). For distances from the neutron star $r < R_A$ magnetic field dominates the motion of matter, which is therefore forced to corotate with the neutron star. For $r > R_A$ the disk matter will move freely in Keplerian orbits. The disk matter enters into the magnetosphere only if the rotation angular velocity of the neutron star is not larger than the Keplerian angular velocity at $r = R_A$.

& van der Hucht (1988), which gives a fit for stellar wind rate as a function of luminosity (L) and surface temperature (T). This relation was used to fit another relation, with the stellar evolution model of Schaller et al. (1992), to get the stellar wind rate as a function of mass of the star. This fit is given by,

$$y = p_\circ + p_1 x + p_2 x^2 + p_3 x^3 \tag{3.14}$$

where y $= \log \dot{M}$, $x = \log$ M, and the values of the constants are $p_\circ = -14.454$, $p_1 = 7.037$, $p_2 = -1.218$, $p_3 = 0.032$.

The accretion radius of the neutron star is taken to be,

$$r_{\mathrm{acc}} = \left(\frac{2G\,M_n}{v_w^2 + c_s^2}\right) \tag{3.15}$$

here, M_n is the mass of the neutron star. The velocity of sound c_s is taken to be negligible compared to the terminal velocity of the wind v_w. The terminal velocity is calculated by the following procedure. For a star in main sequence the Coronal Temperature and the velocity of the stellar wind at the sonic point are given by (Erica Bohm-Vitense 1989),

$$\begin{aligned} T_c &\leq 5.73 \times 10^6 \left(\frac{M}{M_\odot}\right)\left(\frac{R_\odot}{R}\right) \; K \\ v_t &= \sqrt{\frac{2k_B T_c}{m_H}} \end{aligned} \tag{3.16}$$

where M and R are the mass and the radius of the star respectively. The coronal temperature is taken to be half of the value given by the equation given above. The terminal velocity of the stellar wind is taken to be 3 times the value of the velocity at the sonic point. Then, $\dot{m}$ can be easily calculated as $(\dot{M}_c r_{\mathrm{acc}}^2/4a^2)$.

3.2.5 Comparison with the earlier works

Several authors have tried to study the statistical properties of pulsars and binary systems through Monte Carlo simulations similar to the one described in this

Chapter. For instance, Dewey & cordes (1987) have studied the properties of the progenitors of pulsars; Pols *et al.* (1992) have studied the formation of Be stars through close binary evolution, and Pols & Marinus (1994) have studied the evolution of binaries in young open clusters.

Although the procedure followed in this work is essentially the same as in many of these works, the evolution of radio pulsars are modelled in a complete fashion. For instance, parameters like rotational period, magnetic field strength are evolved with some assumed model, and the *observable* distribution of pulsars are calculated by modeling the selection effects completely. This may be considered to be a significant improvement. Moreover, the observed properties of radio pulsars are regarded as observational constraints, rather than the properties of the massive binary systems in the Galaxy. This is because the properties of some species of binaries (for instance Be/X-Ray binaries) are not modelled quite well.

The effect of the impact of the supernova ejecta onto the companion star has been considered by Dewey & Cordes (1987). This effect has been ignored in this exercise since it is not expected to make significant change in the results. The effect of tidal interaction and stellar wind from the stars have also not been considered for this work. However, some of the recent works like Portegies Zwart & Verbunt (1996) consider this effect.

The model followed in this Chapter for computing the fraction of mass lost from the system during the Roche lobe overflow of the primary star was the one suggested in Pols *et* al. (1992) (see section **3.2).** However, Pols & Marinus (1994) have dealt with this problem in a more physical way.

Since the model for the evolution of radio pulsars considered in this Chapter is more robust than the earlier works, the results concerning the "active" neutron star binaries may be considered more reliable.

3.3 The Monte Carlo Simulation

The overall procedure which is followed in this work is to produce a large number of binaries and solitary stars, and find out the end state of these systems with some simplified assumptions described above. The binary parameters like the masses of the two components, and the semimajor axes were generated with respect to the procedure given in section 3.2. The solitary stars and the *primary* stars in binary systems were assumed to follow the Initial Mass Function. The primary stars were generated in the mass range of $6-20M_{\odot}$, and the solitary stars mere generated in the range $8-20M_{\odot}$. Though the threshold mass for neutron star formation in binaries was assumed to be $10M_{\odot}$, binaries were generated with primaries from $6M_{\odot}$. This is to allow for the possibility of having binaries where the secondaries produce neutron stars, with primaries producing white dwarfs. *i.e.,* for binaries with primary mass in the range $6-10M_{\odot}$ if the secondary grows to masses above $10M_{\odot}$ during primary mass transfer, it is assumed that the binary disrupts during the explosion of the secondary, and one solitary neutron star is produced from each of these systems.

With an assumed pulsar birth rate of one in about 75 years (see Chapter 2) the birth rate of these systems (solitary stars plus binaries) is derived to be about one in 50 years or so. The difference in birth rate is due to the fact that many of the binaries may not produce even one neutron star. With an assumed binary-to-singles fraction of 1:1 it is assumed that about 35% of the systems produced are single stars.

The maximum age of pulsars produced in the simulation is assumed to be 200 Myr. The age of a given pulsar was chosen randomly between zero and 200 Myr, with uniform probability.

For pulsars produced by solitary progenitors the initial magnetic field and period are chosen with some assumed distributions, and the lifetime was assigned as described above. The magnetic field was evolved according to equation 3.12. The same procedure was followed for pulsars produced in binaries, but which become solitary after the disruption of the binary during the first supernova explosion. However, if the binary does not disrupt during the first explosion, the first-born neutron star gets spun-down due to the wind from the main sequence companion star. This process may continue as long as the companion is in the main sequence (equation 3.5), or till the corotation radius of the neutron star matches with the Alfvén radius (see Appendix A). The magnetic field during this period is evolved according to equation 3.12 and 3.13. After the spin-down process the pulsar was assumed to be spun-up to the equilibrium period corresponding to the magnetic field of the pulsar at that time. The evolution of the magnetic field after the spin-up is treated identical to that of a solitary pulsar.

The death line is assumed to be $(B_{12}/P^2) = 0.17$, where B_{12} is the field in units if 10^{12} G. If the value of (B_{12}/P^2) is found to be less than 0.2 for any pulsar, it is eliminated from the simulation.

3.3.1 Comparison with Known Samples

To compare the simulated population of solitary pulsars with observed population four parameters are chosen. They are, (i) the rotation period, (ii) time derivative of the rotation period, (iii) magnetic field strength, and (iv) characteristic age. The distribution of aimulated pulsars with respect to these parameters were compared with the observed, by calculating the Kolmogorov-Smirnov probabilities.

As explained in Chapter 2. since the known pulsars are biased by the observational selection effects a subset of the known pulsars which are in principle "detectable" by any one of the 4 surveys namely (1) the U.Mass-Arecibo survey, (2) the Jodrell-I survey, **(3)** the Second Molonglo survey, and (4) the U.Mass-NRAO survey are considered. To reduce the computation time, only the pulsars which are within **3** kpc from the Sun are considered (about 110 in number).

To calculate the model luminosity L_m, we assumed the function given by Stollman (1986),

$$\begin{aligned} \log L_m &= -10.05 + 0.98 \log \frac{B}{P^2}, \qquad \text{for} \;\; \log \frac{B}{P^2} \leq 13 \\ &= 2.71 \qquad\qquad\qquad\qquad\qquad\;\; \log \frac{B}{P^2} > 13 \end{aligned} \tag{3.17}$$

However, one expects that the observed samples are severely biased towards more luminous pulsars. This bias has been modelled by Narayan & Ostriker (1990), who find that the distribution ρ_L of the intrinsic luminosities around the model luminosity can be modelled as,

$$\rho_L = 0.5\lambda^2 e^{-\lambda} \tag{3.18}$$

$$\text{where } \lambda = c\left(\log \frac{L}{L_m} + b\right) \tag{3.19}$$

here the constants b and c are assumed to be 2 and **3,** respectively (this was discussed in Chapter 2).

Although a large number of single pulsars were generated in the simulation, in order to reduce the computation time the simulated population was binned in magnetic field B and period **P,** into a 150 x 150 matrix. Each bin was given a weightage equal to the number of simulated pulsars in that bin. This binned array was compared with the distribution of **P** and B of the known samples by computing Kolmogorov-Smirnov probabilities. About 3000 random positions in the Galaxy (with distance from the Sun d $\leq$ **3** kpc) were selected, and each position was populated with pulsars of various periods and fields (150 x 150 bins). The distance model by Taylor & Cordes (1993) was used to compute the dispersion and scattering smearing for each location of the pulsar. The limiting luminosity value above which the pulsar can be detected by any one of the surveys could be calculated with the knowledge of the distance and the flux limits of the surveys. With the knowledge of this limiting luminosity, and the model luminosity corresponding to a given P and B, the limiting value of λ above which the pulsar can be detected can be calculated by using equation 3.19. The detection probability assigned to the corresponding bin is given by,

$$W_l = \left(0.5\,\lambda^2 + \lambda + 1\right) e^{-\lambda} \tag{3.20}$$

which can be obtained by integrating equation 3.18, from λ to infinity. This procedure enables one to get a distribution in $B - \mathrm{P}$ plane of the observable population. This map was used to calculate K-S probabilities for the distribution of P, B, P and τ_{ch}. Ideally one would like to get the K-S probability in two dimensions. However, since one does not have enough number of known pulsars to describe a smooth distribution in the B $-$ P plane, what is done here is to calculate the K-S probability for four different projections in the B-P plane namely, projection along period, field, time derivative of the period, and the characteristic age. By taking different projections one can recover the lost information to some extent.

3.4 Results

Although we assumed a birth rate of massive stellar systems of one in 50 years, to reduce the computation time the number of systems generated in the simulation

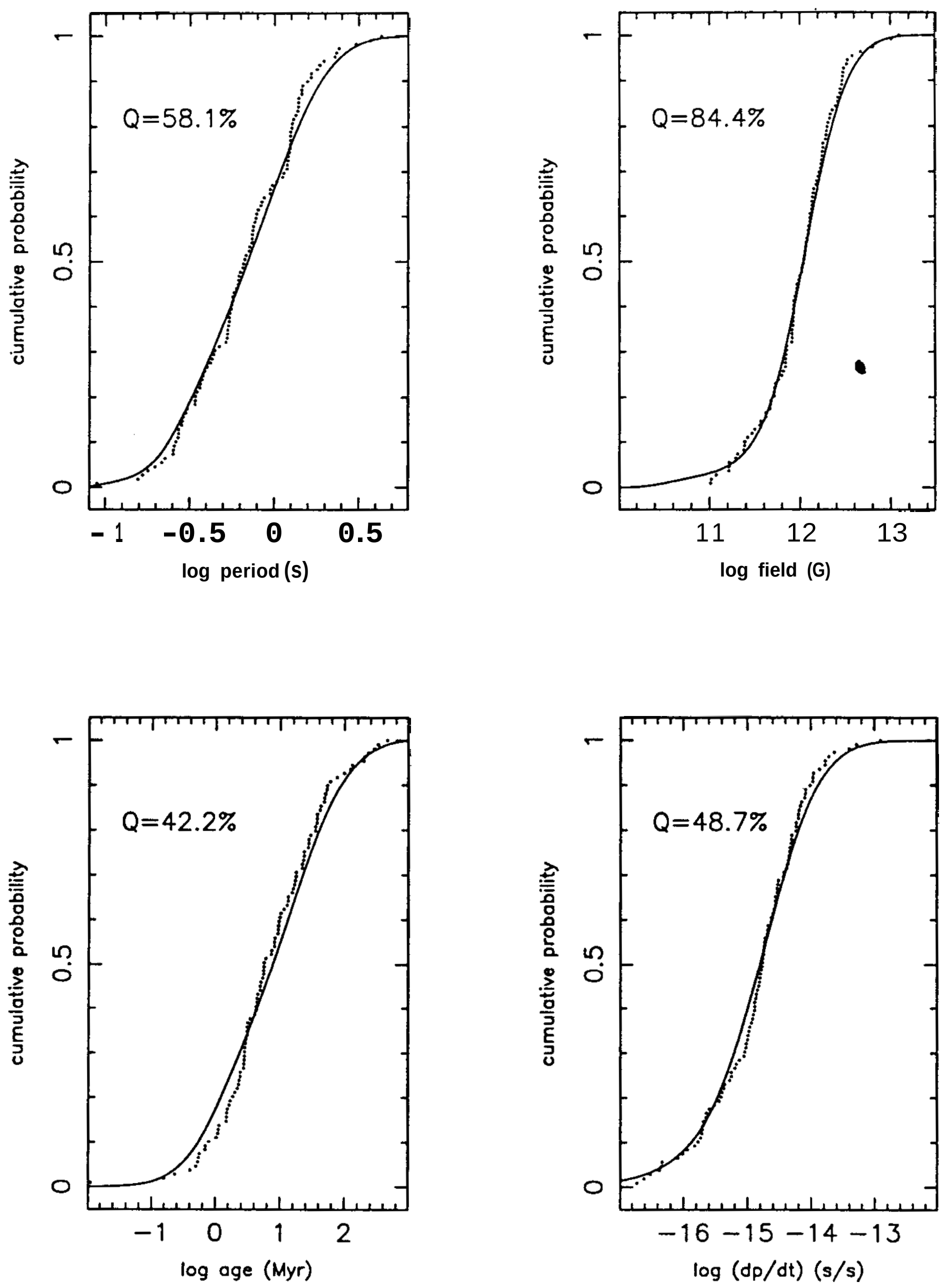

Figure 3.1: The results of the Kolmogorov-Smirnov (K-S) tests. The four plots correspond to rotation period (**P**),magnetic field (B),characteristic age (τ_{ch}) and time derivative of the rotation period (**P**) respectively. The dotted line represents the known samples, and the solid line respresents the simulated population. The corresponding K-S probabilities are also given in each of the plots, represented by Q.

was restricted to a value which corresponds to a third of the birth rate, *i.e.*, one in 130 years. However, to get the correct number of systems in the Galaxy the results were scaled up by a factor of 3.

As mentioned earlier, the stars generated include singles as well as binaries. The number of systems generated was 1.33 x 10^6, out of which about 9 x 10^5 were in binaries. With the HPP velocity distribution (Paczynski 1990; Hansen & Phinney 1996), about 53% of the binaries got disrupted in the first explosion itself. With the Lyne & Lorimer (1993) velocity distribution, about 65% of the binaries got disrupted during the first supernova explosion. Among the binaries, the fraction of binaries generated with $M_1^\circ < 10M_\odot$ is about 66%, where M_1° is the initial primary mass. The number of *active* single pulsars generated in the simulation with a progenitor birth rate of one in 150 is about **2.3** x 10^5.

The maximum K-S probability was achieved for an initial field distribution of sum of two gaussians (in log B), with $\langle\log B\rangle_1 = 12.17$, $\langle\log B\rangle_2 = 12.43$, $\sigma_1 = 0.3$, and $\sigma_2 = 0.36$. The relative weightage of the first gaussian is 0.2 with respect to the second one. **A** combination of two gaussians was chosen for practical convenience (to produce a slightly distorted gaussian), and no physical significance can be attributed to it. The corresponding initial period distribution was a flat distribution in the range of 0.1 – 0.24 sec. Figure 3.1 gives the plots of the K-S tests for the distributions of rotation period (**P**),magnetic field (B),characteristic age (τ_{ch}), and the time derivative of the period ($\dot{\mathbf{P}}$). The corresponding K-S probability values were 58.1%, 84.4%. 42.2% and 48.7%, respectively, which are reasonably good.

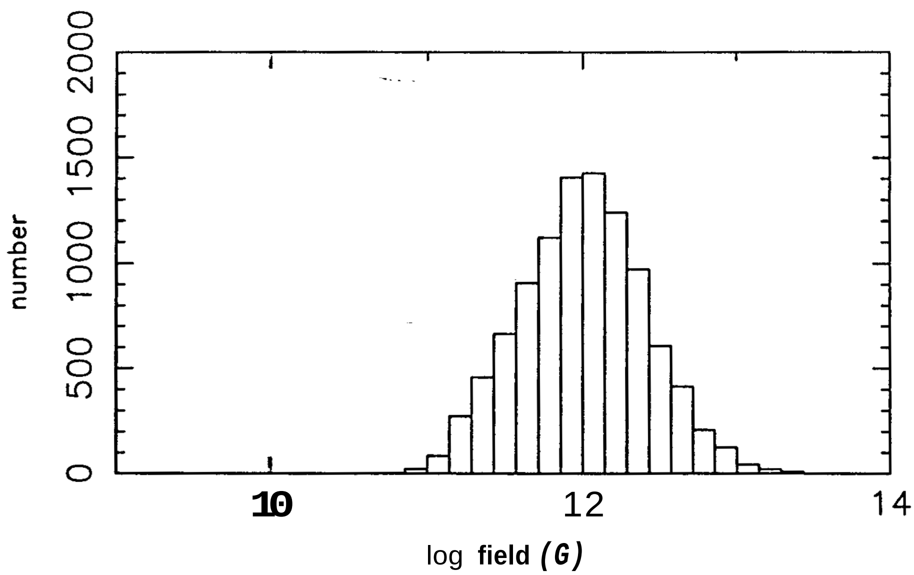

Figure **3.2:** The distribution of magnetic fields of non-recycled pulsars. in the simulation. The non-recycled pulsars are produced by (a) the solitary progenitors, (b) a fraction of binaries **with** $M_1^\circ < 10M_\odot$ (see section **3.3**), (c) the binaries disrupted during the first SNE, (d) the binaries disrupted during the second SNE (only second born pulsars). and (e) a fraction of coalescing binaries which coalesce during the primary star Roche-lobe overflow.

3.4.1 Pulsars from binary systems

One believes that a vast majority of stars we see in the sky may be in binary systems, or multiple systems. Since pulsars are the remnants of massive stars it is natural to expect that a good fraction of pulsars are produced by stars in binary systems. One of the main aims of this simulation is to estimate the fraction of pulsars *processed* (recycled) in binary systems.

As per the assumptions of this simulation, recycled pulsars can be produced by two ways. The first way is by spinning up a neutron star by accretion from the companion, and the second way is by coalescing binaries, *i.e.,* if the orbital energy during the spiral-in phase is not enough to expell the envelope of the companion, the neutron star spirals into the companion star, and coalesces with its *core.* In this process the system is assumed to leave behind only one neutron star. According to Bhattacharya & van den Heuvel (1991), this pulsar will be a recycled pulsar. However, if the binary coalesces during the primary mass transfer itself it is assumed that the binary leaves behind only one ordinary pulsar (not a recycled one).

The second column of the table 3.1 gives the number of solitary pulsars produced by various types of progenitors.

Injection

The concept of injection was introduced in Chapter 2, and discussed in detail. To recall, Vivekanand & Narayan (1981), and Phinney & Blandford (1981) came to a conclusion that not all pulsars are born spinning rapidly like Crab pulsar. Indeed, a considerable fraction of pulsars may be born with periods of the order of a few hundreds of milliseconds or so. Although this has been questioned by many authors, further statistical studies like Narayan (1987), Narayan & Ostriker (1990)

Progenitor	number of pulsars	pulsars with $\log B < 11.5$
A	96961	11019
B	26429	2922
C	67032	7598
D	3140	425
E	3671	427
F	32717†	13012
A–F	229950	35403

Table 3.1: *A : from single progenitors, B : from binaries with* $M_1^\circ < 10M_\odot$, *C : from binariks disrupted during the first explosion, D : first-born PSRs from binaries disrupted in the second explosion, E : second-born PSRs from binaries disrupted in the second explosion, and* **F** *: from coalescing binaries.* The numbers given given in the table correspond to an assumed progenitor birth rate of one in 150 years. To get the *true* number (*i.e.,* corresponding to the progenitor birth rate of one in 50 years, each of these numbers must be multiplied by 3. The third column gives the number of pulsars with $\log B < 11.5$. The significance of this is discussed in section 3.4.1. The last row of the table gives the total number of pulsars from all progenitors.

† Out of this 32717, 14566 pulsars are recycled.

and Deshpande *et al.* (1995) have found evidence in favour of injection. From the detailed current analysis discussed in Chapter 2 one came to the conclusion that the injection occurs predominantly in two field ranges ($B = 10^{10.5} - 10^{11.5}$G and $B = 10^{12} - 10^{12.6}$G). The interpretation given was that the injection of pulsars with relatively low fields is to be identified with recycled pulsars from intermediate mass range binaries, and the high field injection with recycled pulsars from massive binaries. One of the aims of this simulation is to see if the conventional recycling mechanism can support this hypothesis.

As mentioned earlier, as per the initial assumptions there are two ways of producing recycled pulsars – by the usual way of spin-up due to accretion of matter in binaries, and by coalescing binaries. Also, it is assumed that all the binaries which survive after the first explosion go through the spiral-in phase, and the change in semimajor axis is calculated with equation 3.6. Figure 3.2 gives the distribution of the magnetic fields of ordinary (non-recycled) pulsars produced in the simulation. This must be compared with figure 3.3, which gives the distribution of magnetic fields of recycled pulsars. The top panel is for pulsars produced through the usual recycling scenario, and the bottom panel is for pulsars produced through coalescing binaries. In the case of binaries with a neutron star and a massive star, the left-over main sequence life time of the companion after the first explosion is too short to spin-down the neutron star significantly (here it should be noted that in the field decay mechanism assumed the field decay is directly related to the extent to which the neutron star is spun-down). Consequently the amount of field decay is not significant. That is why the distribution given in the first panel of figure **3.3** is not significantly different from figure **3.2.** However, in the case of binaries with relatively low mass companions the left-over main sequence life time is long enough to slow down the neutron star to a period of about 1000 seconds or so. Therefore, one can expect a considerable amount of field decay. This is clearly seen in the second panel of figure **3.3.** However, the exact distribution in this case can not be believed literally since we have assumed that all binaries (irrespective of the mass-ratio and the semimajor **axis)** go through the spiral-in phase. Although this assumption may be valid for systems with extreme mass-ratio, in the case of systems with q $\sim$unity this assumption may fail.

Fraction of injected pulsars and their birth rate

Table 3.1 gives the details of pulsars produced in the simulation. Various rows give the number of pulsars from different types of binaries (corresponding to a

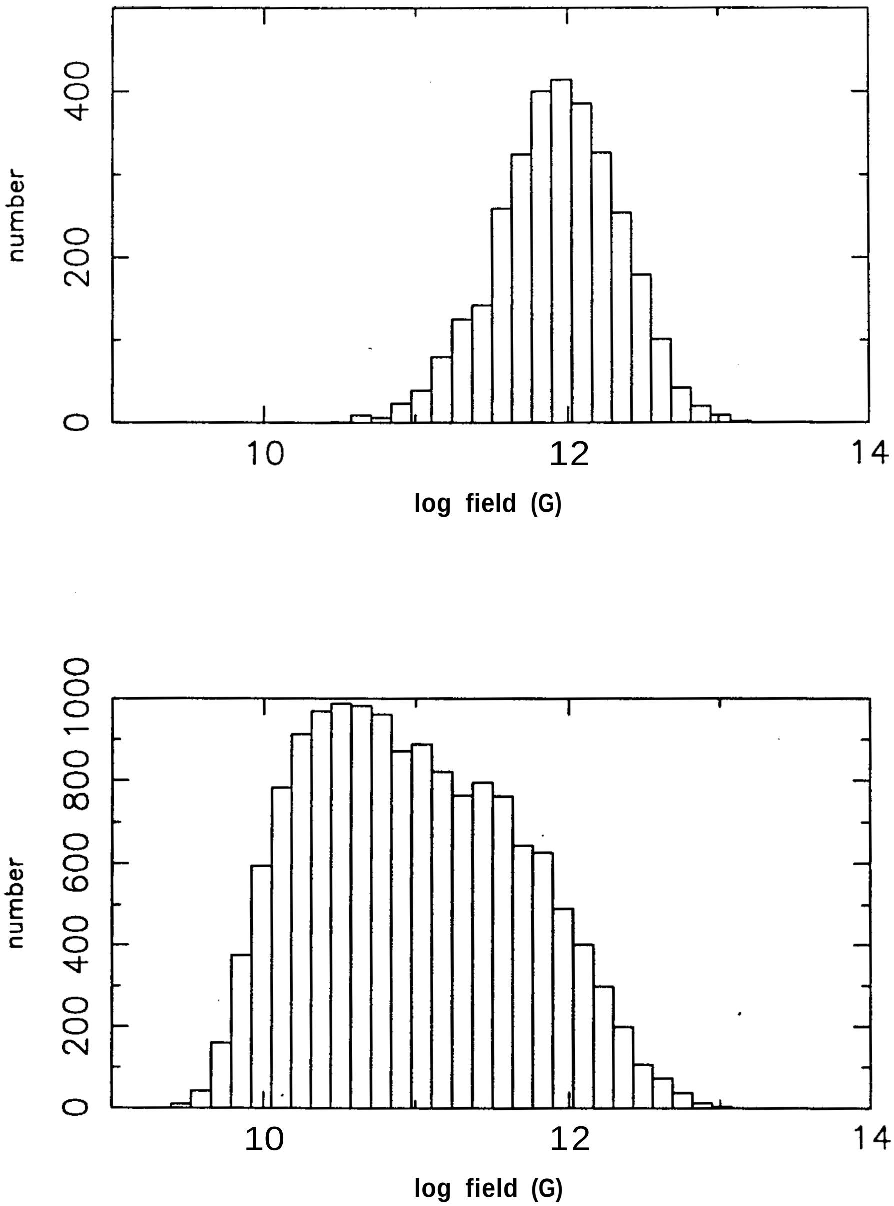

Figure **3.3:** The distribution of magnetic fields of recycled pulsars in the simulation. The top panel corresponds to the pulsars produced by conventional recycling, and the bottom panel corresponds to the recycled pulsars produced from coalescing binaries. See section 3.4.1 for more details.

progenitor birth rate of one in 150 years). The third column gives the number of pulsars with $\log B(G) < 11.5$. The rows which give the number of recycled pulsars are Row-D (which gives the number of first-born pulsars from binaries which get disrupted during the second supernova explosion), and Row-**F** (which gives the number of pulsars from coalescing binaries). However, one must keep in mind that only a fraction of the number of pulsars given in Row-**F** are recycled (as mentioned in the footnote of the table). This gives us the fraction of recycled pulsars produced in the simulation to be about 7.7% of the total number of pulsars produced. If one looks at the number of recycled pulsars with fields greater than $\log B = 11.5$, the fraction of recycled pulsars is only 1.9%.

Now, let us try to estimate the birth rate of pulsars with $\log B < 11.5$. The average characteristic age of these pulsars in the simulation turns out to be about $\sim$ 300 Myr. As given in the third column of table 3.1 the number of pulsars with $\log B < 11.5$ is 35403 (one has to multiply this number by 3 to get the number of pulsars corresponding to the progenitor birth rate of one in 50 years). With the knowledge of the average characteristic age and the total number of pulsars one can try to estimate the approximate birth rate, and this turns out to be about $(1/3000)\mathrm{yr}^{-1}$. This must be compared with the birth rate of these pulsars estimated in Chapter 2 – $(1/5000)\mathrm{yr}^{-1}$. Keeping in mind the assumption we made about the spiral-in, this discrepancy is not significant.

The average characteristic age of pulsars with $\log B > 11.5$ is about 50 Myr. Since the number of pulsars with $\log B > 11.5$ is much more than the number of pulsars with $\log B$ less than 11.5, we may approximate the average cliaracteristic age of the whole population to be about 50 Myr. With this knowledge! the birth rate of the simulated pulsar population in the whole range of $\log B$ come to about $1/72\mathrm{yr}^{-1}$, which matches with the value derived in Chapter 2. one in 75 ± 15 years.

As mentioned above the fraction of recycled pulsars in the total simulated population is about 7.7%. Now, let us try to estimate the fractional birth rate of these recycled pulsars. The number of recycled pulsars produced by the usual scenario (first-born pulsars from binaries disrupted during the second supernova explosion) is 3140, and the number of recycled pulsars from coalescing binaries is 14566 (see the footnote of table 3.1). Out of this 14566, 3651 pulsars have $\log B > 11.5$. With the knowledge of the average characteristic age of pulsars with $\log B$ greater and less than 11.5, the birth rate of these recycled pulsars is estimated to be about **3.7%** of the total birth rate of pulsars.

From an analysis of the pulsar current we earlier estimated the upper limit to the fraction of pulsars processed in binary systems to be about 10 – 15%. The results mentioned above seem to suggest that the fraction of recycled pulsars is only about $\sim 8\%$. Even among the pulsars with $\log B < 11.5$ (total of 35403), only 11340 were recycled, which is about 35% of the number of pulsars with $\log B < 11.5$.

When the kick velocity distribution was assumed to be that of Lyne & Lorimer (1993), then the total number of recycled pulsars came down to 12501, which is only 5.3% of the total population. The implication of these results will be discussed in section **3.5.**

3.4.2 Double neutron star binaries

Apart from computing the fraction of pulsars processed in binary systems, this simulation was used to compute the formation rate and the number of ***active*** NS-NS binaries (where at least one neutron star is alive as pulsar) in the Galaxy, and to compute the merger (due to gravitational radiation) rate of SS-SS binaries. This section summarises these results.

Active double neutron star binaries

With the HPP velocity distribution the number of *active* (atleast one of the neutron stars is alive as pulsar) double neutron star binaries produced in the simulation (corresponding to the progenitor birth rate of one in 50 years) is 6867. Out of this, the first-born neutron star was active in 4545 binaries, and the second-born neutron star was active in 5115 binaries. Both the neutron stars were active in 2793 binaries. When the velocity distribution was changed to Lyne & Lorimer distribution, the total number of double neutron star binaries came down to about 2300. These numbers are much less than the numbers derived by Narayan *et al.* (1991). The possible reasons for this discrepancy will be discussed in section 3.5. In section 3.5 we will also try to compare the distribution of magnetic fields and orbital periods with the known sample.

Formation and Merger Rate of double neutron star binaries

Finding out the merger rate of double neutron star binaries is much more difficult than finding out the number of *active* double neutron star binaries, for one is not sure whether the population is in steady state or not! Therefore, for this part of the simulation it was assumed that the maximum age of the objects is the age of the Galaxy, instead of the previously assumed 200 Myr. Moreover, for the purpose of estimating the merger rate whether or not the neutron stars are *active* is irrelevant. Following the same procedure as mentioned in section 3.3 the orbital period of all double neutron star binaries produced in the simulation were stored, along with the information of their age (age was chosen randomly from zero to 13 Byr, with uniform probability). Then the change in the orbital period due to the emission of gravitational radiation was calculated for each binary. Figure 3.4 gives the distribution of orbital periods of double neutron star binaries. The first

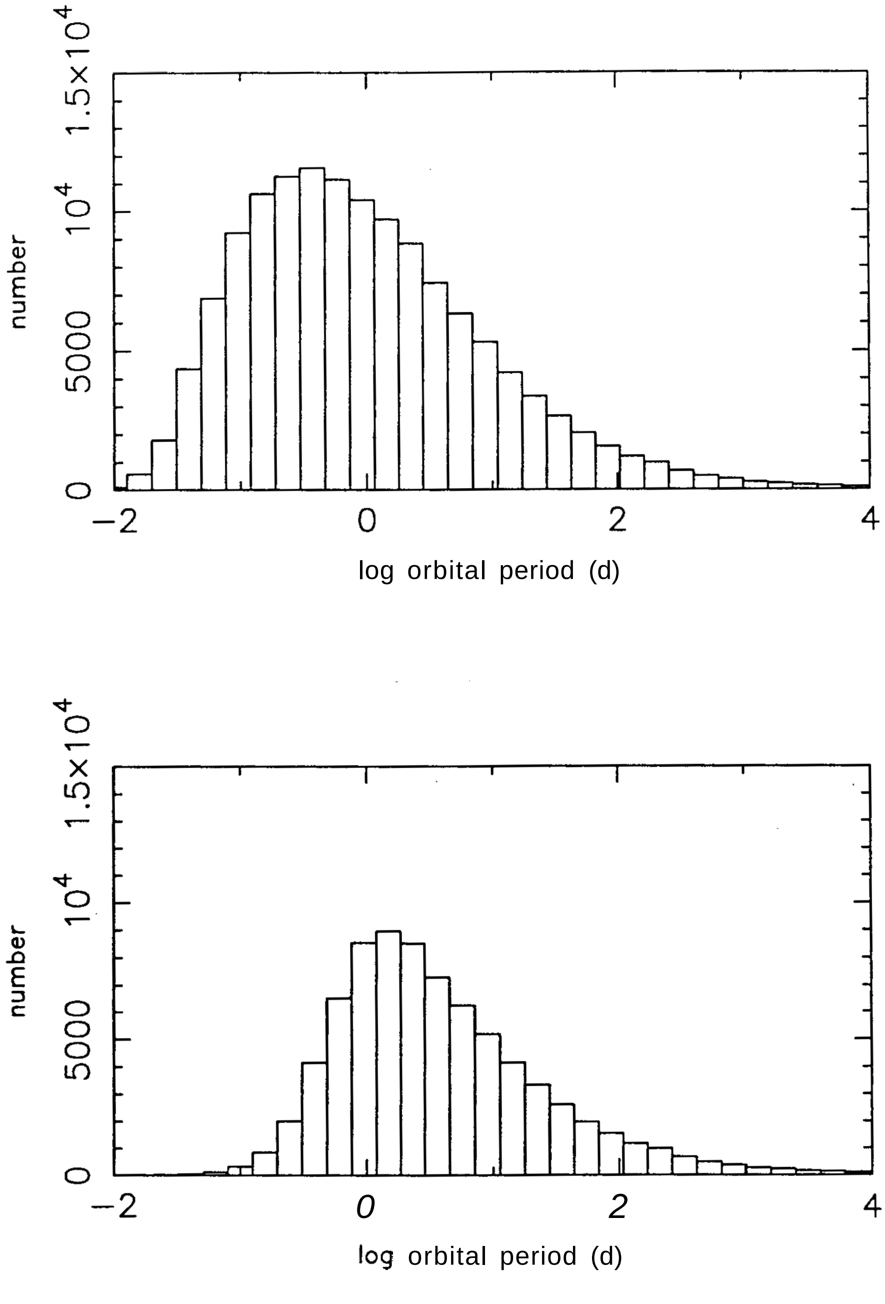

Figure **3.4:** The distribution of orbital periods of double neutron star binaries produced in the simulation. The top panel shows the distribution of their orbital periods at their birth, and the bottom panel shows the distribution after evolving the system for roughly the age of the Galaxy ($\sim$ 13Byr.). As one can see, the shorter orbital period binaries merge due to the emition of gravitational radiation.

panel gives the distribution of orbital periods at birth, and the second panel gives the distribution after taking into account of the change in the orbital period due to the gravitational radiation. The eccentricity of the binaries was assumed to be zero while calculating the change in the orbital period due to the emission of gravitational radiation.

With the kick velocity distribution given by equation 3.9, the formation rate of double neutron star binaries turns out to be about 10^{-4} per year, *i.e.,* , 100 binaries per million years. This should be compared with the formation rate of $10^{-4.5}$/yr deduced by Narayan et al. (1991), and $(2-4) \times 10^{-4}$/yr by van den Heuvel (1992).

The merger rate of these binaries was found to be about 4.4×10^{-5}/yr (assuming circular orbits). This should be compared with $10^{-6} z_\circ$/yr by Narayan et al. (1991), and $(4-8) \times 10^{-5}$/yr by van den Heuvel (1992). A conservative estimate by Phinney (1991) gives a value of about a few times 10^{-6}/yr. Here, $z_\circ$ is the scale height of these objects in the Galaxy.

When the kick velocity distribution was assumed to be Lyne & Lorimer distribution, the formation rate reduced to 3.3×10^{-5}/yr, and the merger rate came down to 2×10^{-5}/yr.

Effect of changing parameters

Since some of the assumptions in the simulation are quite uncertain, it is important to see how sensitive the formation and merger rate for these assumptions. We assumed two different models for the Initial hlass-Ratio Function (IMRF) and the mass-loss fraction. For the IMRF, the first model is given by equation 3.1, and the second model is a uniform distribution, from $q = 0.1$ to $q = 1$. For the mass-loss fraction, the first is the one described in section 3.2. and the second is a completely conservative evolution. The most favoured models are the first models.

When the IMRF was changed to the second model the formation rate increased by about 40%, where as the merger rate went up by about 25%.

When the mass-loss model was changed to the second model, both the formation rate and the merger rate increased by about a factor of four.

3.5 Discussion

The variation in the K-S probability with different initial seed for generating random numbers is seen to be about a percent.

The properties that we have chosen to vary are the distribution of initial rotation period and the magnetic field of the pulsars. The objects were not evolved in the Galactic potential to get their spatial distribution in the Galaxy.

The magnetic field decay time scale of the crust of the pulsar is assumed to be 100 Myr. Though in principle this could have been one of our free parameters, since many of the earlier works concluded that the field decay time scale of pulsars is much longer (see Bhattacharya et *al.* 1992), we decided to assume a long decay time scale. The decay time scale of the core is assumed to be infinity, since it is believed to be superconducting.

Helium stars, during the later stages of core helium burning and during helium shell burning, undergo a considerable radius expansion (Habets 1985, 1986). In tight binaries this may lead to a second spiral-in, in which a good fraction of the helium-rich envelope of the helium star is lost. However, this effect is not considered for this simulation. If one include this effect, it might lead to some increase in the merger rate of NS-NS systems.

From the statistical analysis described in Chapter 2 we derived an upper limit to the fraction of pulsars injected into the main population. This fraction was about 10 – 15%. We hypothesised that the injected pulsars may be the recycled pulsars from massive and intermediate mass range binaries in the Galaxy. If one takes this as the actual fraction of injected pulsars, then this must be compared with the recycled pulsar fraction in the simulation. As mentioned in section 3.4.1 with the assumption of HPP velocity distribution we find that only about 8% can be identified with recycled pulsars. With Lyne & Lorimer velocity distribution this number is about 5.3%. The reason for this discrepancy is the following. A very good fraction of binaries get disrupted during the first explosion itself. Also, quite a few binaries (with extreme mass-ratios) coalesce during the primary star Roche-lobe overflow. There are two ways of resolving this problem: one is to say that only part of the injected pulsars are injected from binaries, and the others are born with long initial periods; Alternatively, the kick velocity distributions assumed in this simulation are biased against low velocities. This could be due to some observational selection effects (which biases against observing low velocity pulsars) which one may not have modelled well. After this work was completed we became aware of an independent study by Portegies Zwart & Verbunt (1996). Although their assumptions differ from ours in detail, their overall conclusions about the fraction of pulsars recycled in binaries is very similar to what is described here.

The number of ***active*** double neutron star binaries in the Galaxy is found to be about a few thousands (see section 3.4.2). This is much smaller than the number derived by Narayan et al. (1991). According to Narayan et al. this number is about $35000 z_\circ$, where $z_\circ$ is the scale height of these objects in kpc. In their opinion $z_\circ$ is of the order of a few kpc. A similar number has been suggested for binary systems like PSR 1913+16 by van den Heuvel (1992). The reason for the discrepancy is not clear. However, the analysis of Narayan et *al.* is based on only three pulsars (PSR 1913+16, 1534+12, 2303+46), and the scale factor of 1534+12 is much larger than the scale factors of the other two pulsars. Thus their result is dominated by one pulsar.

pulsar	Rotation period (ms)	log B (G)	Orbital period (d)	eccentricity
B1913+16	59.03	10.36	0.323	0.617
B1534+12	37.90	9.99	0.421	0.274
B2303+46	1066.37	11.90	12.339	0.658

Table 3.2: Parameters of the three known disc double neutron star binaries.

The distribution of orbital periods of the ***active*** double neutron star binaries is not different from the distribution at birth (see the first panel of figure 3.4). This is expected because the average time taken by these binaries to merge due to the emission of gravitational radiation is quite longer than their average life time as pulsars. As one can see, the distribution of orbital periods peaks at a period of about $\log P_{orb} \sim -0.5$ ($\approx \mathbf{0.3}$ days). The orbital periods of the known double neutron star binaries are listed in table 3.2. Though one can not do a satisfactory job in comparing the simulated distribution with the observed distribution (since we have only three known samples), it can be seen that the orbital periods of the known samples are not far from the peak of the distribution.

The distribution of magnetic fields of pulsars in the double neutron star binaries is given in figure 3.5. As one can see, the fields of these pulsars have not decayed significantly. This is due to the fact that the left-over main sequence life time of the massive secondary star after the primary overflow is not long enough to slow down the neutron star to long periods (see section 3.2.4). If it is true that the magnetic fields of the first-born pulsars in these massive binaries are not

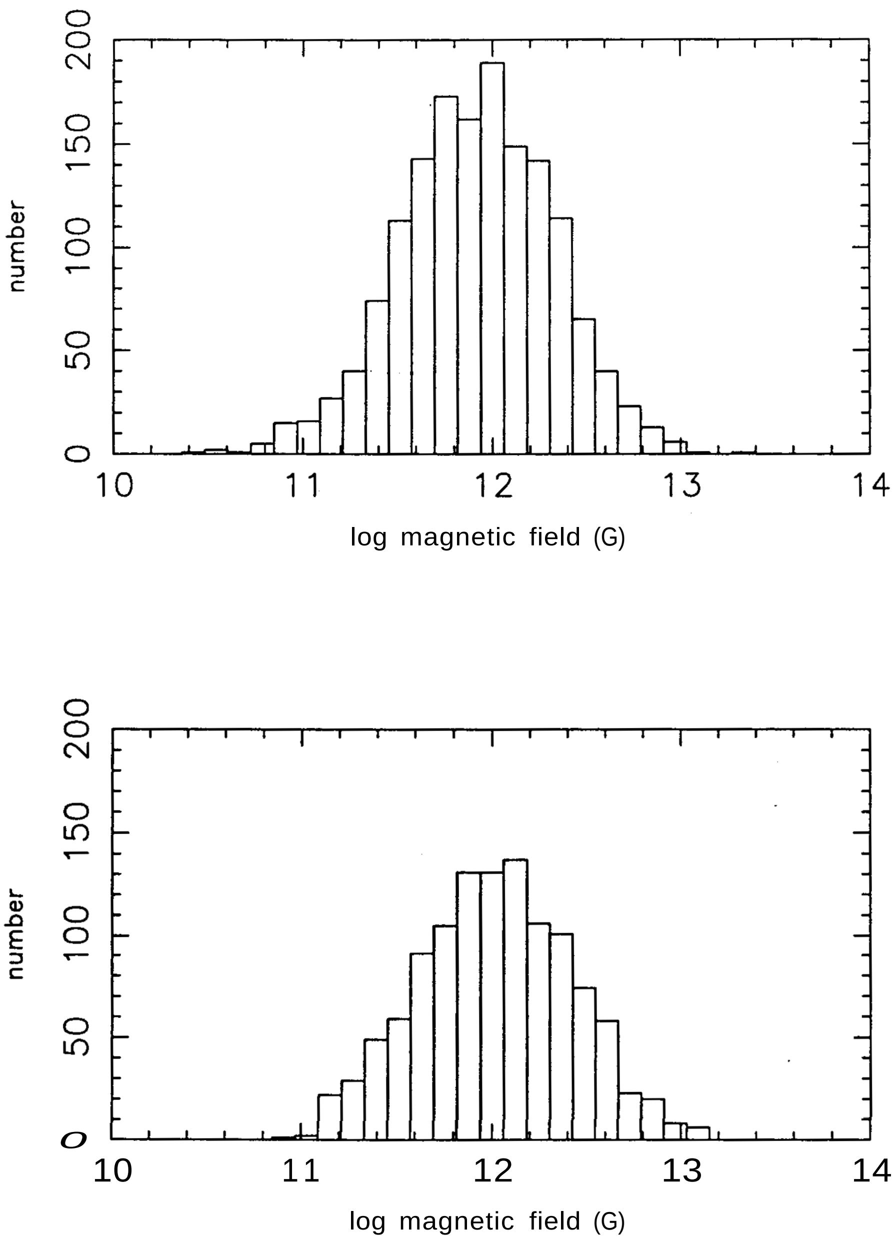

Figure 3.5: The distribution of magnetic fields of pulsars in the double neutron star binaries. The top panel corresponds to the distribution of magnetic fields of the first-born pulsars, and the bottom panel corresponds to that of the second-born pulsars.

significantly lower than the second-born pulsars, in general, it may be difficult for one to say whether a pulsar is recycled or not (B1913+16 and B1534+12 may be exceptions).

While calculating the merger rate we have assumed that the eccentricity of the double neutron star binaries is zero. However, the the three Galactic double neutron star binaries seem to have eccentric orbits. If one assumes that all NS-NS binaries have an eccentricity like that of PSR 1913+16, the merger rate increases by a factor of about 1.5 to 2.

If one takes the merger rate to be about 2×10^{-5}/yr for our Galaxy, one can try to estimate the expected rate of mergers from which some advanced detectors like LIGO can hope to detect gravitational radiation. This would assume that the merger rate for our Galaxy is roughly the same as that of the external Galaxies. If one takes the galaxy density to be $10^{-2}h^3$ Mpc^{-3} where h is the Hubble constant in terms of 100 km sec^{-1} Mpc^{-1} (Kirshner *et al.* 1983; Phinney 1991), then the NS-NS merger rate out to a distance of $\sim 200\text{Mpc}/h$ turns out to be about 6 events/year. The number calculated by Narayan *etal.* (1991) is about one per year.

Summary

The main results from this chapter are the following.

- If the asymmetric kick velocity distribution is assumed to be the distribution given by Hansen & Phinney (1996), or Lyne & Lorimer (1993), the fraction of recycled pulsars may be only about $5 - 8\%$.

- The number of ***active*** (where at least one of the neutron stars is alive as pulsar) double neutron star binaries in the Galaxy is about a few thousands, and this number is much less than the number given by the earlier works such as Narayan et al. (1991). Their formation rate in the Galaxy is estimated to be about 10^{-4} yr^{-1}.

- The merger rate of double neutron star binaries (due to the emission of gravitational radiation) in the Galaxy is about $2-4 \times 10^{-5}$ yr^{-1}. Assuming a galaxy density in the local universe, the extrapolated event rate upto a distance of about 200 Mpc may be about a few events per year.